Provided for non-commercial research and education use.
Not for reproduction, distribution or commercial use.

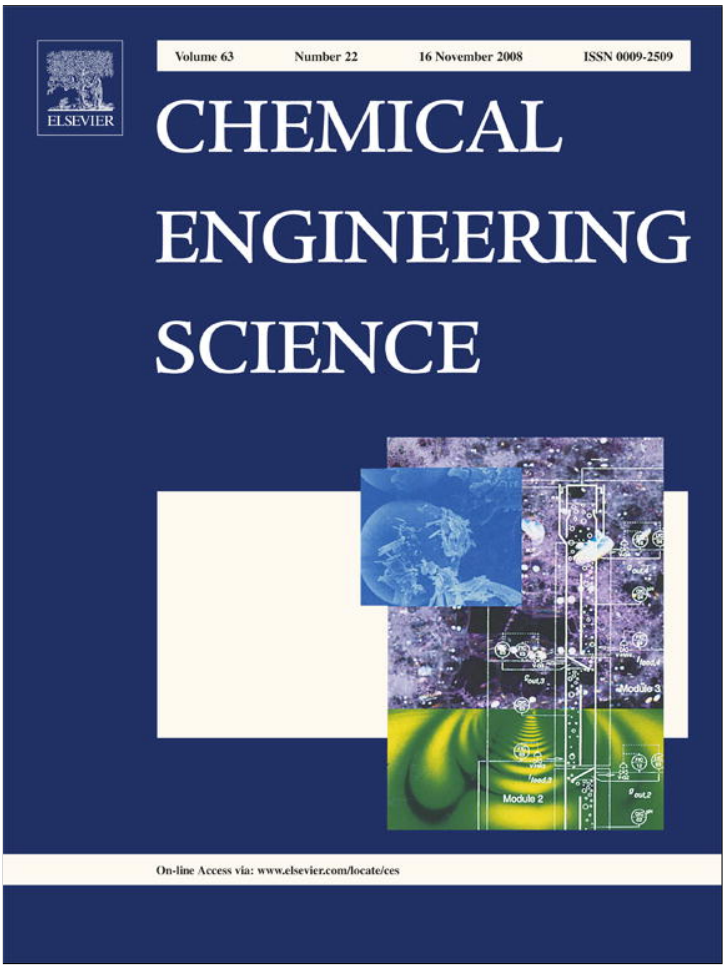

This article appeared in a journal published by Elsevier. The attached copy is furnished to the author for internal non-commercial research and education use, including for instruction at the authors institution and sharing with colleagues.

Other uses, including reproduction and distribution, or selling or licensing copies, or posting to personal, institutional or third party websites are prohibited.

In most cases authors are permitted to post their version of the article (e.g. in Word or Tex form) to their personal website or institutional repository. Authors requiring further information regarding Elsevier's archiving and manuscript policies are encouraged to visit:

http://www.elsevier.com/copyright

Author's personal copy

Chemical Engineering Science 63 (2008) 5425 – 5433

Contents lists available at ScienceDirect

Chemical Engineering Science

journal homepage: www.elsevier.com/locate/ces

Optimal mechano-electric stabilization of cardiac alternans

Stevan Dubljevic[a,*], Panagiotis D. Christofides[b]

[a]Cardiovascular Research Laboratories, David Geffen School of Medicine, University of California, Los Angeles, CA 90095, USA
[b]Department of Chemical and Biomolecular Engineering, University of California, Los Angeles, CA 90095, USA

ARTICLE INFO

Article history:
Received 15 February 2008
Received in revised form 23 July 2008
Accepted 1 August 2008
Available online 6 August 2008

Keywords:
Cardiac mechano-electric feedback (MEF)
Dissipative parabolic PDEs
LQR
State/output feedback control

ABSTRACT

Alternation of normal action-potential morphology in the myocardium is a condition with a beat-to-beat oscillation in the length of the electric wave which is linked through electromechanical coupling to the cardiac muscle contraction, and is believed to be the first manifestation of the onset of life threatening ventricular arrhythmias and sudden cardiac death. In this work, the effects of electrical and mechanical stimuli are utilized in alternans annihilation problem. Electrical stimuli that alter the action-potential morphology are represented by a pacer located at the domain's boundary, while mechanical stimuli are distributed within the spatial domain and affect the action potential by altering intracellular calcium kinetics. Alternation of action potential is described by the small amplitude of alternans parabolic partial differential equation (PDE). Spatially uniform unstable steady state of the alternans amplitude PDE is stabilized by optimal control methods through boundary and spatially distributed actuation. Mixed boundary and spatially distributed actuation is manipulated by a linear quadratic regulator (LQR) in the full-state-feedback control structure and in a compensator design with a finite-dimensional Luenberger-type observer, and it achieves exponential stabilization in a finite size tissue cable length. The proposed control problem formulation and the performance and robustness of the closed-loop system under the proposed linear controller are evaluated through simulations.

© 2008 Elsevier Ltd. All rights reserved.

1. Introduction

Sudden cardiac death and ventricular fibrilation are believed to be linked to the alternation of the electric activity of the myocardium. Electric activity in the heart is the consequence of propagation of electric waves caused by the exchange of ionic species between intracellular and extracellular spaces which is reflected in changes in the membrane potential of the myocardium cells. Electric wave propagation in myocardium belongs to the class of transport-reaction processes which are characterized by significant spatial variations due to the coupling of underlying diffusion and nonlinear dynamics phenomena. Hence, it has been shown that when cardiac tissue is stimulated at short pacing rates, the duration of electrical excitation varies from beat to beat, and it is manifested as a variation in the action potential duration (APD). These beat-to-beat oscillations are referred to as "alternans", see Fig. 1.

Annihilation of detrimental alternans may represent an effective antiarrhythmic strategy and it has been addressed in the theoretical studies of Echebarria and Karma which demonstrated that alternans can be abolished only in a small portion of tissue by applying modulated feedback gain which perturbs the fixed pacing period and can be produced by consecutive APD measurements at the pacing site (Echebarria and Karma, 2002b). Control of this type belongs to the class of boundary control realizations since the pacing site is at the boundary of the domain which undergoes stabilization. Current assessment is that the applied pacing control stabilization of alternans is not successful due to limited ability of the applied pacing boundary input to alter the APD length away from the pacing site which has been demonstrated by theoretical and experimental works (Echebarria and Karma, 2002b; Christini et al., 2006; Lin and Dubljevic, 2007; Dubljevic et al., 2008).

An independent from pacing way to change the cell's electrical activity is to apply mechanical stimuli. In recent experimental and theoretical studies (Kohl et al., 1999; Solovyova et al., 2004; Kohl and Ravens, 2003; Calaghan et al., 2003; Bers, 2001), it has been demonstrated that stretch-induced changes of myocardium cell length alter the electric activity through stretch-activated channels and by modulation of intercellular calcium kinetics. Namely, the kinetics of intercellular calcium is primarily responsible for the link among electrical and mechanical properties of the cell since binding of the intercellular calcium ions with contractile proteins provides a local mechanism of mechanic contractile act. Motivated by these findings, in this work stretch-based mechanical perturbation,

* Corresponding author. Tel.: +1 310 794 3658.
E-mail addresses: stevand@seas.ucla.edu (S. Dubljevic), pdc@seas.ucla.edu (P.D. Christofides).

0009-2509/$ - see front matter © 2008 Elsevier Ltd. All rights reserved.
doi:10.1016/j.ces.2008.08.001

Author's personal copy

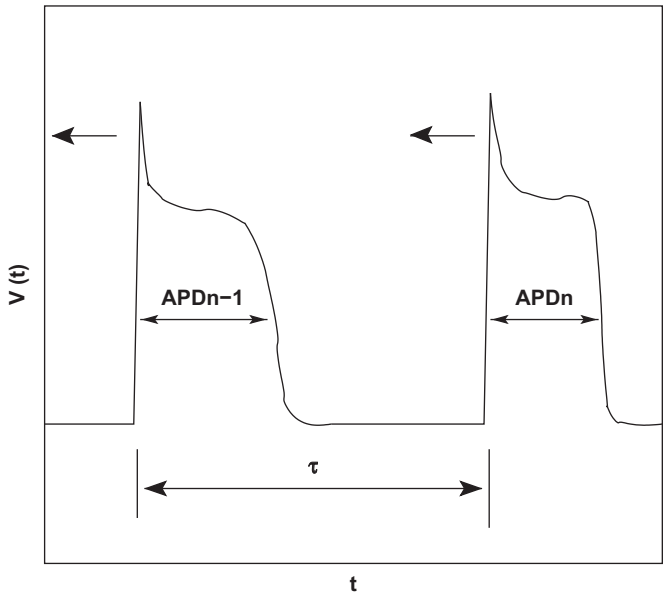

Fig. 1. Schematic time course of the transmembrane potential at a point along the cable with APD alternans, where the amplitude of alternans $a(\zeta,t)$ is defined as $a(\zeta,n)=(\mathrm{APD}_{n,\zeta}-\mathrm{APD}_{n-1,\zeta})(-1)^n$ with n being the beat number and $t=n\tau$, where τ is the basic beat length.

which does not belong to the type of superthreshold stimuli, alters the intercellular calcium kinetics by which the cells electrical activity is modulated (Calaghan et al., 2003). The stretch-based mechanical perturbation is spatially distributed within the myocardium tissue, and when paired with boundary applied pacing, it can provide a mixed boundary–spatially distributed mechano-electric perturbation that may, by mechanisms of mechano-electric feedback (MEF), lead to successful cardiac alternans annihilation. Boundary actuation is represented by the alternation of the pacing period at the boundary of the domain and it is realized by placing an electrode at the cardiac muscle. Spatially distributed actuation is associated with MEF, as a result of stretch-based mechanical perturbations on the tissue through stretch-activated and stretch-modulated ionic currents among which the calcium current is the most important one in the mechano-electric coupling mechanism. Spatially distributed mechanical stretch actuation can be easily realized by sewing the micro-electro-mechanical-based built patch to the epicardial myocardial tissue. Therefore, a mixed boundary and spatially distributed mechano-electric control actuation formulation is proposed in this work, as a new promising way to cardiac alternans annihilation therapy since two independent ways of interaction with cardiac tissue by electrical and mechanical stimuli are more capable to tame the heart into regular action-potential propagation. This work is appealing from a clinical point of view since the mechanical actuation of the heart muscle, which has not been addressed from the annihilation of alternans perspective, is investigated.

A small amplitude of alternans equation that was derived by Echebarria and Karma (2002b) obeys the form of parabolic partial differential equations (PDEs) that model diffusion–convection–reaction processes (Ray, 1981; Cross and Hohenberg, 1993). Typically, systems described by parabolic PDEs admit an abstract evolutionary form on an appropriate functional space, and in the case of linear parabolic PDEs, the spatial differential operator is characterized by a spectrum that can be partitioned into a finite (possibly unstable) slow part and an infinite-dimensional stable fast complement (Friedman, 1976). Hence, the traditional approach to control parabolic PDEs is to stabilize the unstable slow modal states via feedback, while the infinite-dimensional stable modal complement remains stable under the applied feedback control structure.

Within the theory of control of parabolic PDEs, this work focuses on the subset of mixed boundary/distributed control problems for linear parabolic PDEs. In this area, significant research has been carried out in the works of Fattorini (1968), Triggiani (1980), Curtain and Zwart (1995), Christofides (2001) and Emirsjlow and Townley (2000), wherein necessary conditions for the stabilization under state- and output-feedback control have been defined. More recent results on the boundary control of distributed parameter systems include the use of singular functions for identification and control (Chakravarti and Ray, 1999), boundary control of nonlinear distributed parameter systems by means of static and dynamic output-feedback regulation (Byrnes et al., 2004), development of boundary feedback control laws based on the backstepping methodology (Boskovic et al., 2001) and model predictive methodology that includes input and state constraints in the boundary/distributed control design (Dubljevic and Christofides, 2006a; Dubljevic et al., 2006). Building on these already developed control methods, the issue of stabilization of cardiac alternans by boundary and distributed applied actuation needs to be explored as a possible antiarrhythmic strategy.

In this paper, mixed boundary and distributed stabilization of small amplitude of the alternans equation described by a linear parabolic PDE by optimal control methods is demonstrated. Linear parabolic PDE of amplitude of alternans is defined as a mixed abstract boundary/distributed control problem in a well-defined functional space. The analysis demonstrates that the spatial operator of the amplitude of alternans PDE is a Sturm–Liouville type operator, which possesses a few unstable modes that can be stabilized by means of boundary and distributed feedback control. Namely, only few unstable modes are exponentially stabilized by a full-state-feedback linear quadratic regulator (LQR), while the remaining infinite-dimensional complement remains stable under the applied feedback controller. In the case of output-feedback control, a Luenberger-type observer is integrated with the LQR control law to achieve exponential stabilization of the alternans amplitude PDE. In simulation studies, the relevant model of the Beeler–Reuter cardiac cell is considered in order to obtain parameters of the amplitude of alternans equation. Successful stabilization by means of optimal boundary/distributed control of small amplitude of alternans is demonstrated and the effect of measurement noise and uncertainty/nonlinearities on the performance of the proposed controller is examined.

2. Preliminaries

When cardiac myocytes are subjected to an electrical stimulus of sufficient magnitude, the affected cells undergo a quick depolarizing upstroke followed by a slow repolarization phase that returns cells to their resting membrane potential (see Fig. 1). The observed electrical phenomena, which are due to the exchange of ionic species among extracellular and intracellular space, are known as the action potential. Additionally, diffusive coupling between cells allows for an action potential from the pacing site to propagate into surrounding tissue, thus bringing about a wave of voltage depolarization (voltage upstroke) and subsequent slow repolarization (voltage downstroke to the resting potential) in the entire system.

The system used in our study is a one-dimensional (1D) homogeneous cell cable of length $L=2.5$ cm, described by the following equation:

$$\frac{\partial V(\zeta,t)}{\partial t}=D\frac{\partial^2 V(\zeta,t)}{\partial \zeta^2}-I_{\mathrm{ion}}(\zeta,t)/C_m \tag{1}$$

Author's personal copy

with the following boundary conditions:

$$\frac{\partial V(0,t)}{\partial \zeta} = V_p(t), \quad \frac{\partial V(L,t)}{\partial \zeta} = 0 \tag{2}$$

$I_{\text{ion}}(\zeta,t)$ is the membrane current with equations taken from the Beeler and Reuter (1977) model. The Beeler–Reuter model is the first relevant physiological model that accounts for calcium dynamics in the cardiac myocyte. $V_p(t)=I_{\text{stim}}/C_m$ is the voltage stimulus supplied by the pacer. The basic pacing period is $\tau=288$ ms, the electric diffusion constant is $D=1.0\text{e}^{-3}$ cm^2/ms and the membrane capacitance is set at $C_m = 1\ \mu\text{F/cm}^2$. Voltage evolution in the cable equation is calculated using a finite difference approximation of Eq. (1) with mesh size $\Delta\zeta = 0.025$ and standard explicit Euler time integration scheme with step size $\Delta t=0.1$ ms. Beeler–Reuter model of cardiac cell is used to determine all relevant parameters in the amplitude of alternans equation (Eq. (5)). The APD is calculated from the length of time during which the cell membrane potential is above the threshold value (-40 mV) and the diastolic time interval ($\text{DI} = \tau - \text{APD}$) is taken to be the length of time during which the cell membrane potential is below the given threshold value for the given n-th beat (see Fig. 1). When the applied pacing period becomes sufficiently short, subsequent stimuli will result in cardiac alternans, which are manifested by an alternating pattern of long and short APDs. The amplitude of alternans, $a_n(\zeta)$, is defined as

$$a(\zeta,n) = (\text{APD}_{n,\zeta} - \text{APD}_{n-1,\zeta})(-1)^n \tag{3}$$

That is, the beat-to-beat variation in the APD in the pattern long–short L–S–L–S–L … yields the non-negative amplitude of alternans along the cable which is defined as the difference between the APD of the current beat and of the previous beat. This convenient definition allows the use of discrete APD measurements for mapping the continuous voltage evolution into $a_n(\zeta)$, where $n = t/\tau$. Stabilization of alternans in the cardiac cells cable described by Eqs. (1)–(2) can be achieved by coupling boundary and spatially distributed feedback control. The boundary control component of our control protocol is established by measuring the difference between the current APD and previous APD at the pacing site. This difference is used as the input to modulate the pacing period at the pacing site. In other words,

$$T_{n(\zeta=0)} = \tau + \gamma(\text{APD}_{n(\zeta=0)} - \text{APD}_{n-1(\zeta=0)}) \tag{4}$$

where τ is the basic pacing cycle period and γ is the adjustable feedback gain for APD alternation of the basic pacing period at a pacing site. T_n is the applied pacing period.

On the basis of slow beat-to-beat variation of the amplitude of alternans and functional relation given by Eq. (3), the equation which describes the small amplitude oscillations of the APD was developed by Echebarria and Karma (2002a,b), and for 1D $\zeta \in [0,l]$ case, the amplitude of alternans parabolic PDE takes the following form:

$$\tau_c \frac{\partial a(\zeta,t)}{\partial t} = D_a^2 \frac{\partial^2 a(\zeta,t)}{\partial \zeta^2} - w\frac{\partial a(\zeta,t)}{\partial \zeta} + \sigma a(\zeta,t) - g a(\zeta,t)^3 - \frac{1}{\Lambda}\int_0^{\zeta} a(\bar{\zeta},t)\,\mathrm{d}\bar{\zeta} + h\sum_{i=1}^{n} b_{di}(\zeta)u_{di}(t) \tag{5}$$

$$\frac{\partial a(0,t)}{\partial \zeta} = a(0,t) + u(t)$$

$$\frac{\partial a(l,t)}{\partial \zeta} = 0 \tag{6}$$

$$y(t) = \int_0^l c(\zeta)a(\zeta,t)\,\mathrm{d}\zeta \tag{7}$$

The parameters D_a and w are taken to be $D_a \approx \sqrt{D * \text{APD}_c}$ and $w \approx 2D/c_v^*$, where D is the voltage diffusion among the cells in the ionic model (Beeler and Reuter, 1977), APD_c is the APD evaluated at the bifurcation point, τ_c is the basic pacing cycle length at the bifurcation point, and c_v^* is the propagation speed of the wave front at the bifurcation point at which alternans start to emerge (Echebarria and Karma, 2002b). The parameter σ is the growth rate of alternans at the onset of period doubling oscillations in the APD, while the parameter g is the nonlinear stabilizing contribution (see Echebarria and Karma, 2002a, for exact derivation of σ and g). The integral term in Eq. (5) reflects the contribution of the perturbation of the basic pacing cycle length on the amplitude of alternans. The parameter h represents the correlation that relates the changes in the intracellular calcium dynamics due to mechanical perturbations with respect to the alternans amplitude. In this analysis, the exact length and timing of the stretch-activated excitation is not provided and the assumption is that stretch actuation is mainly manifested by the modulation of the intracellular calcium dynamics which is reflected in the changes in the APD morphology.

The amplitude of alternans PDE of Eqs. (5) and (6) is linearized around the spatially uniform unstable steady state ($a(\zeta,t)=0$). We assume that alternans are slowly varying from the beat to beat in the proximity of the bifurcation point. We consider the case when alternans start to emerge and since alternans dynamics is described by a nonlinear bistable equation, a first approximation is given by the linearized amplitude of alternans equation. Further, the integral term in Eq. (5) that reflects the contribution of the perturbation of the basic pacing cycle length on the amplitude of alternans, in the context of control of relevant cardiac tissue size is negligible and can be neglected (the parameter $\Lambda \approx 45$–50 cm, Echebarria and Karma, 2002b). See the Simulation section for results, demonstrating that the use of the linearized model for controller design is adequate in the sense that a controller that is designed on the basis of the linearized PDE stabilizes the full model of Eqs. (5) and (6).

In the ensuing text, the linearized amplitude of alternans PDE is considered and it can be formulated as a mixed abstract boundary/distributed control problem:

$$\dot{a}(t) = \mathscr{F}a(t) + \mathscr{B}_d u_d(t), \quad t \geqslant 0, \quad a(0) = a_0 \tag{8}$$

$$\mathscr{B}a(t) = u(t)$$

$$y(t) = \mathscr{C}a(t)$$

where $\mathscr{F} : \mathscr{D}(\mathscr{F}) \subset \mathscr{W} \mapsto \mathscr{W}$, $\mathscr{B}_d \in \mathscr{L}(U_d, \mathscr{W})$, $\mathscr{B} : \mathscr{D}(\mathscr{B}) \subset \mathscr{W} \mapsto U$ satisfies $\mathscr{D}(\mathscr{F}) \subset \mathscr{D}(\mathscr{B})$, and U, U_d and $\mathscr{W}([0,l];t)$ are well-defined Sobolev spaces, with the state $a(\cdot,t) = \{a(\zeta,t), 0 \leqslant \zeta \leqslant l\} \in \mathscr{W}([0,l];t)$ (Curtain and Zwart, 1995), t is the time variable, $u(t) \in \mathbb{R}$ is the control input at the boundary, and $u_d(t)$ is the spatially distributed input. $L_2(0,l)$ denotes the Hilbert space of measurable square-integrable real-valued functions $f : [0,l] \to \mathbb{R}$, $\int_0^l |f(\zeta)|^2\,\mathrm{d}\zeta < \infty$, with weighted inner product and norm on $L_2(0,l)$, defined by $(f,g)_{\eta,L_2} = \int_0^l \mathrm{e}^{-\eta\zeta} f(\zeta)g(\zeta)\,\mathrm{d}\zeta$ and $\|f\|_2 = \sqrt{(f,f)_{\eta,L_2}}$. Associated with Eq. (8) is the operator $\mathscr{F}$ which is given by

$$\mathscr{F}\phi(\zeta) = \left[D_a^2\frac{\mathrm{d}^2}{\mathrm{d}\zeta^2} - w\frac{\mathrm{d}}{\mathrm{d}\zeta} + \sigma\right]\phi(\zeta) \tag{9}$$

with the domain defined by

$$\mathscr{D}(\mathscr{F}) = \{\phi(\zeta) \in L_2(0,l) : \phi(\zeta), \phi(\zeta)', \text{ are abs. cont.}, \mathscr{F}\phi(\zeta) \in L_2(0,l), \text{ and } \phi(l)' = 0\} \tag{10}$$

Author's personal copy

while the input operator of spatially distributed control actuation is given by

$$\mathscr{B}_d u_d(t) = h\sum_{i=1}^{n} b_{di}(\zeta)u_{di}(t) \tag{11}$$

where $b_{di}(\zeta) = (1/2\varepsilon)1_{[\zeta_{d_i}-\varepsilon,\zeta_{d_i}+\varepsilon]}(\zeta) \in L_2(0,l)$ (this notation means that $b_{di}(\zeta) = 1/2\varepsilon$ for $\zeta_{d_i} - \varepsilon \leqslant \zeta \leqslant \zeta_{d_i} + \varepsilon$ and $b_{di}(\zeta) = 0$ elsewhere). The output operator is defined by a sensor function as $c(\zeta) = (1/2\varepsilon)1_{[\zeta_c-\varepsilon,\zeta_c+\varepsilon]}(\zeta) \in L_2(0,l)$, and it is given by

$$y(t) = (c(\zeta), a(\zeta,t)) = \mathscr{C}a(t) \tag{12}$$

The boundary operator $\mathscr{B} : L_2(0,l) \mapsto \mathbb{R}$ and its domain are given by

$$\mathscr{B}\phi(\zeta) = \frac{\mathrm{d}\phi(0)}{\mathrm{d}\zeta} - \phi(0) \quad \text{with } \mathscr{D}(\mathscr{F}) \subset \mathscr{D}(\mathscr{B}) \tag{13}$$

In order to define a mixed abstract boundary/distributed control problem it is necessary to introduce a new operator $\mathscr{A}$ which is defined by

$$\mathscr{A}\phi(\zeta) = \mathscr{F}\phi(\zeta) \quad \text{and}$$

$$\begin{aligned}\mathscr{D}(\mathscr{A}) &= \mathscr{D}(\mathscr{F}) \cap \ker(\mathscr{B})\\ &= \{\phi \in L_2(0,l) : \phi(\zeta), \phi(\zeta)' \text{ are abs. cont.},\\ &\quad \mathscr{A}\phi(\zeta) \in L_2(0,l), \phi'(0) = \phi(0) \text{ and } \phi'(l) = 0\}\end{aligned} \tag{14}$$

where $\mathscr{A}$ is the infinitesimal generator of a strongly continuous semigroup on $\mathscr{W}$. An assumption made here is that there exists a function $B(\zeta)$ so that for all $u(t)$, $Bu(t) \in \mathscr{D}(\mathscr{F})$ and the following holds:

$$\mathscr{B}Bu(t) = u(t), \quad u(t) \in U \tag{15}$$

The existence of B together with the assumption that the input $u(t) \in \mathbf{C}^2([0,t];U)$ and $u_d(t) \in \mathbf{C}^1([0,t];U_d)$ are sufficiently smooth, yield the following well-posed abstract differential equation:

$$\begin{aligned}&\dot{p}(t) = \mathscr{A}p(t) + \mathscr{F}Bu(t) - B\dot{u}(t) + \mathscr{B}_d u_d(t)\\ &p(0) = p_0 \in \mathscr{D}(\mathscr{A})\\ &y(t) = \mathscr{C}p(t) + \mathscr{C}Bu(t)\end{aligned} \tag{16}$$

which has a well-defined mild solution due to the boundedness of linear operators B and $\mathscr{F}B$, and due to the fact that $\mathscr{A}$ is the infinitesimal generator of a C_0-semigroup. Eqs. (16) and (8) are related by the following transformation $p(t) = a(t) - Bu(t)$. As the abstract evolutionary equation of Eq. (16) includes in its expression a derivative of the control term, it is reformulated on the extended state space $\mathscr{W}^e := \mathscr{W} \otimes U$, as $a^e(t) = [u(t)\ p(t)]'$ and together with $\tilde{u}(t) = \dot{u}(t)$ yields

$$\begin{aligned}&\dot{a}^e(t) = \begin{pmatrix} 0 & 0 \\ \mathscr{F}B & \mathscr{A} \end{pmatrix} a^e(t) + \begin{pmatrix} I & 0 \\ -B & \mathscr{B}_d \end{pmatrix} \begin{pmatrix} \tilde{u}(t) \\ u_d(t) \end{pmatrix}\\ &a^e(0) = [u(0)\ \ p(0)]' = a_0^e\\ &y^e(t) = [\mathscr{C}B\ \ \mathscr{C}]a^e(t)\end{aligned} \tag{17}$$

The operator $\mathscr{A}^e = (0\ \ 0; \mathscr{F}B\ \ \mathscr{A})$ with domain $\mathscr{D}(\mathscr{A}^e) = \mathscr{D}(\mathscr{A}) \otimes U$ is the infinitesimal generator of a C_0-semigroup on $\mathscr{W}^e$. The Riesz spectral operator $\mathscr{A}$ generates a C_0-strongly continuous semigroup $\mathscr{T}(t)$ given by

$$\mathscr{T}(t) = \sum_{n=0}^{\infty} \mathrm{e}^{\lambda_n t}(\cdot, \phi_n(\zeta))\psi_n(\zeta) \tag{18}$$

so that $\sup_{n\geqslant 1} Re(\lambda_n) \leqslant \infty$, where $\lambda_n\{n \geqslant 1\}$, are simple eigenvalues of $\mathscr{A}$, and $\phi_n(\zeta)$ and $\psi_n(\zeta)$ are the eigenfunctions of $\mathscr{A}$ and $\mathscr{A}^*$, respectively, so that the inner product $(\phi_n(\zeta), \psi_m(\zeta))_{L_2} = \delta_{nm}$ holds.

The eigenvalue problem of the Sturm–Liouville operator given by Eqs. (9) and (14) can be easily solved (Curtain and Zwart, 1995). Namely, the operator $\mathscr{A}$ is given, for any function in the domain $\mathscr{D}(\mathscr{A})$, by

$$\mathscr{A}\phi(\cdot) = \frac{1}{\rho(\cdot)}\frac{\mathrm{d}}{\mathrm{d}\zeta}\left[p(\cdot)\frac{\mathrm{d}\phi}{\mathrm{d}\zeta}(\cdot)\right] + q(\cdot)\phi(\cdot) \tag{19}$$

where $\rho(\zeta) := \mathrm{e}^{-(w/D_a^2)\zeta}$, $p(\zeta) := D_a^2\rho(\zeta)$, $q(\zeta) := \sigma$ which are continuously differentiable functions on $[0,l]$. The spectrum of eigenvalues of the operator $\mathscr{A}$ is $\Omega(\mathscr{A})$ and consists of isolated eigenvalues with finite multiplicity and it is given by

$$\lambda_n = \sigma - D_a^2\left[\alpha_n + \frac{w^2}{4D_a^4}\right], \quad 0 < \alpha_n < \alpha_{n+1}, \ \ n \geqslant 1 \tag{20}$$

where α_n is the solution to the following transcendental equation:

$$\tan(\sqrt{\alpha}L) = \frac{\sqrt{\alpha}}{\alpha - \dfrac{w}{2D_a^2}\left[1 - \dfrac{w}{2D_a^2}\right]} \tag{21}$$

while the eigenfunctions for all $n \geqslant 1$ are given by

$$\phi_n(\zeta) = A_n\mathrm{e}^{(w/2D_a^2)\zeta}\left[\cos(\sqrt{\alpha_n}\zeta) + \left(1 - \frac{w}{2D_a^2}\right)\frac{1}{\sqrt{\alpha_n}}\sin(\sqrt{\alpha_n}\zeta)\right] \tag{22}$$

and the adjoint eigenfunctions by $\psi_n(\zeta) = \phi_n^*(\zeta) = \phi_n(\zeta)\mathrm{e}^{-(w/D_a^2)\zeta}$, where A_n are nonzero constants which are calculated by the orthogonality condition $(\phi_n(\zeta), \phi_m^*(\zeta))_{w/D_a^2,L_2} = \delta_{nm}$. The semigroup $\mathscr{T}(t)$ growth bound is given by $\omega_0 = \sup_{n\geqslant 1} Re(\lambda_n) \leqslant \infty$ and the following characterization of the operator $\mathscr{A}$ that generates the operator $\mathscr{T}(t)$ is given by the Hille–Yoshida theorem (Curtain and Zwart, 1995), $\|\mathscr{T}(t)\| \leqslant M\mathrm{e}^{\omega_0 t}$ for a $M > 0$.

Remark 1. The approximate controllability of mixed boundary/distributed controlled system of Eq. (17) can be assured by checking that the following condition holds for all $n \geqslant 1$:

$$\mathrm{rank}[(\mathscr{F}B(\zeta) - \lambda_n B(\zeta), \phi_n(\zeta))_{w/D_a^2,L_2}\ \ (\mathscr{B}_d, \phi_n(\zeta))_{w/D_a^2,L_2}] = 1 \tag{23}$$

where the first entry corresponds to the boundary actuation related condition of approximate controllability, while the second entry refers to approximate controllability of spatially distributed actuation. In the same vein, the condition of approximate observability for the boundary/distributed controlled problem holds if the $\mathrm{rank}[(\mathscr{C}(B(\zeta) + I), \phi_n(\zeta))] = 1$ holds for $n \geqslant 1$. The approximate controllability and observability conditions of boundary/distributed controlled system are transformed from their standard forms due to the boundary transformation (Curtain and Zwart, 1995).

3. Optimal controller design

The operator $\mathscr{A}^e$ spectrum is partitioned into a finite-dimensional unstable part $\Omega^+(\mathscr{A}^e)$ and an infinite-dimensional stable complement $\Omega^-(\mathscr{A}^e)$, $\Omega(\mathscr{A}^e) = \Omega^+(\mathscr{A}^e) \cup \Omega^-(\mathscr{A}^e)$. The finite-dimensional LQR problem for the finite-dimensional state given by $a_u^e(t) = [u(t)\ p_u(t)]'$ and boundary/distributed actuation $\bar{u}(t) = [\tilde{u}(t)\ u_d(t)]'$ is formulated in the following form:

$$\min_{\bar{u}} \quad J(a_u^e(0); \bar{u}) = \int_0^{\infty} (a_u^e(t)'Qa_u^e(t) + \bar{u}(t)'R\bar{u}(t))\,\mathrm{d}t \tag{24}$$

$$\text{s.t.} \quad \dot{a}_u^e(t) = \mathscr{A}_u a_u^e(t) + \mathscr{B}_u\bar{u}(t) \tag{25}$$

where $\mathscr{A}_u$ and $\mathscr{B}_u$ are matrices that correspond by their dimensions to the dimensions of an unstable eigenspace $\Omega^+(\mathscr{A}^e)$, and Q and R

Author's personal copy

are positive semidefinite and positive definite matrices, respectively. The resulting linear optimal controller is $\bar{u}(t) = -\frac{1}{2}R^{-1}\mathscr{B}_u' P a_u^e(t) = -\mathscr{K} a_u^e(t)$, where P is a positive definite solution to the LQR-Algebraic Riccati Equation (Willems, 1971):

$$0 = \mathscr{A}_u' P + P\mathscr{A}_u + Q - P\mathscr{B}_u R^{-1}\mathscr{B}_u' P \tag{26}$$

Standard Lyapunov-based analysis of stabilization of unstable modes $a_u^e(t)$ by LQR state feedback can be demonstrated by considering the following standard control Lyapunov function (CLF), $V(t) = a_u^e(t)' P a_u^e(t)$, so that

$$\begin{aligned}\dot{V}(t) &= \frac{\mathrm{d}}{\mathrm{d}t}[a_u^e(t)' P a_u^e(t)] \\ &= a_u^e(t)'(\mathscr{A}_u' P + P\mathscr{A}_u - P\mathscr{B}_u R^{-1}\mathscr{B}_u' P) a_u^e(t) \\ &= -a_u^e(t)' Q a_u^e(t) < 0\end{aligned} \tag{27}$$

From Eq. (27), it can be concluded that the unstable modes are optimally stabilized and due to the cascaded interconnection between unstable and stable modal states, once the unstable states are stabilized under the stabilizing feedback law, $a_u^e(t) \to 0$ and $\bar{u}(t) \to 0$, the stable infinite modal states evolution is only driven by the zero-input dynamics which renders exponential stability of the infinite-dimensional closed-loop system. The approximate controllability of the mixed boundary/distributed control system can be assured by checking that the condition given by Eq. (23) holds. In the formulation of the LQR control law given by Eqs. (24) and (25) the associated weights given by Q and R matrices represent weights on the state evolution $p(t)$, control input evolution $u(t)$ and $u_d(t)$, and derivative of boundary control input $\tilde{u}(t)$. The first diagonal term in the matrix Q represents the weight that is associated with $u(t)$, while the remaining nonzero terms are weights on modal states $p(t)$. The term R consists of the weight on the derivative of the input and weights on the distributed control input.

In the case where state-feedback control cannot be realized, it is natural to extend the controller synthesis by incorporating an observer in the feedback structure. A state observer of the Luenberger type is considered (Dochain, 2001). The assumption of approximate observability is made (Curtain and Zwart, 1995), and the Luenberger observer is constructed as

$$\dot{\hat{a}}_u^e = \mathscr{A}_u \hat{a}_u^e(t) + \mathscr{B}_u \tilde{u}(t) - \mathscr{L}(y(t) - \mathscr{C}_u \hat{a}^e(t)) \tag{28}$$

where $\mathscr{C}_u$ is a matrix of appropriate dimensions corresponding to the dimensions of the unstable eigenspace $\Omega^+(\mathscr{A})$ and the number of measurement sensors. Finally, under the assumption of exponential stabilizability and detectability of $(\mathscr{A}_u, \mathscr{B}_u)$ and $(\mathscr{A}_u, \mathscr{C}_u)$, respectively, there exist $\mathscr{K}$ and $\mathscr{L}$ so that $\mathscr{A}_u + \mathscr{B}_u\mathscr{K}$ and $\mathscr{A}_u + \mathscr{C}_u\mathscr{L}$ are exponentially stable. The resulting output-feedback controller enforces exponential stability in the linearized finite-dimensional closed-loop system.

Remark 2. It is of importance to address the issue of noise in the framework of the compensator design. Propagation of the electric wave front in the myocardium is approximately around 65 cm/s which implies that a small noise introduced at the boundary where the control is applied may generate perturbations that will propagate and form a standing wave solution, which is usually, in a crude approximation, a linear combination of the eigenfunctions of the modes of the unstable eigenspace. This effect is indeed observed in the experimental realization of pacing protocols that measure the amplitude of alternans at the pacing site and apply a self-referencing gain feedback modulation of the basic pacing period at the pacing site (Christini et al., 2006). In simulation studies in the following section, it is demonstrated that the noise level that will produce a substantial deviation of the state $a(n, \zeta)$ from zero under a compensator in use in the closed loop is very low.

Remark 3. Although the optimal stabilization of unstable modes of the finite-dimensional subsystem via state-feedback control achieves the exponential stabilization of infinite-dimensional state, it neglects the influence of the feedback law on the remaining set of eigenmodes in a sense that the feedback law may excite higher modes of the operator $\mathscr{A}$ and produce high gain that amplifies the higher modes evolution. This phenomenon is referred to as spillover effect and it is analyzed in Balas (1978) and Hagen and Mezic (2003). This phenomenon is reflected in a possible high excursion of the state from the spatially uniform equilibrium state $a(\zeta, t) = 0$ far from the boundary where the control is applied before the state $a(\zeta, t)$ eventually settles to zero.

Remark 4. One of the important issues arising in the realization of boundary/distributed control actuation in the cardiac relevant size tissue is the issue of the optimal placement of distributed actuation. The optimal placement of the distributed actuators, which can be explored in light of the work delinated in Antoniades and Christofides (2001) and Armaou and Demetriou (2006) should be incorporated in a complementary manner with the life threatening anatomical and structural features of a sick cardiac tissue in order to lead physicians to the "best possible site" for location of the distributed control actuators.

Remark 5. There is a number of clinically important factors related with sick cardiac tissue. For example, scars on the cardiac muscle due to myocardial infraction, or ischemic (lacking of oxygen) parts of the heart due to the smoking or other coronary related diseases (high cholesterol that induces reduced blood supply to the heart muscle), or some other structural problems in the heart geometry, represent important factors that impinge on the design of the type of the controller that uses boundary/distributed mechano-electric-based actuation. These features that can be assessed by the physician with noninvasive techniques may be represented as constraints in the controller synthesis, and the natural selection of the optimal controller synthesis would be model predictive control (MPC) in the context of the parabolic PDEs which is capable of input and state constraints inclusion (Dubljevic et al., 2006; Dubljevic and Christofides, 2006b). However, this controller realization will be highly dependent on the correct reconstruction of the state of the amplitude of alternans which must be obtained in real time on the chip that is embedded in the implantable cardiac device. Having this in mind, this will lead to a difficult controller framework to be realized in practice, while on the other hand, precomputed and easily implementable LQR (LQG) compensator is more desirable since the mild stabilization of the alternans is achievable with this type of control.

4. Simulation study

The parabolic PDE of Eqs. (5) and (6) is considered. The parameters D_a, w, σ, h, g and Λ are obtained from the Beeler–Reuter model of a cardiac cell (Beeler and Reuter, 1977). The critical basic pacing cycle at the bifurcation point where the onset of alternans emerges is at $\tau_c = 275$ ms. The following values of $D_a^2 = 0.1732\,\mathrm{cm}^2$ with voltage diffusion being $D = 10^{-3}\,\mathrm{cm}^2/\mathrm{ms}$, $w = 0.0107$ cm and $\sigma = \log(8)$, and $h = -0.0201$ ms are calculated. The parameters associated with the nonlinear and integral term are $\Lambda = 49$ and $g = 0.0739$. The spectrum of the operator $\Omega(\mathscr{A})$ is calculated using Eqs. (20) and (21) and it reveals different distributions of eigenvalues for different cable lengths. Namely, for $l = 2.5$ that is considered as a case study length of the cable under the optimal control law of Eqs. (24) and (25), the first three eigenvalues of the operator $\mathscr{A}$ are unstable ($\lambda_1 = 0.007429$, $\lambda_2 = 0.0061607$, $\lambda_3 = 0.0031352$), while the remaining infinite eigenvalues are stable, see Fig. 2. The eigenfunctions corresponding to the first three eigenvalues are given in Fig. 3. It can been seen from Fig. 2

Author's personal copy

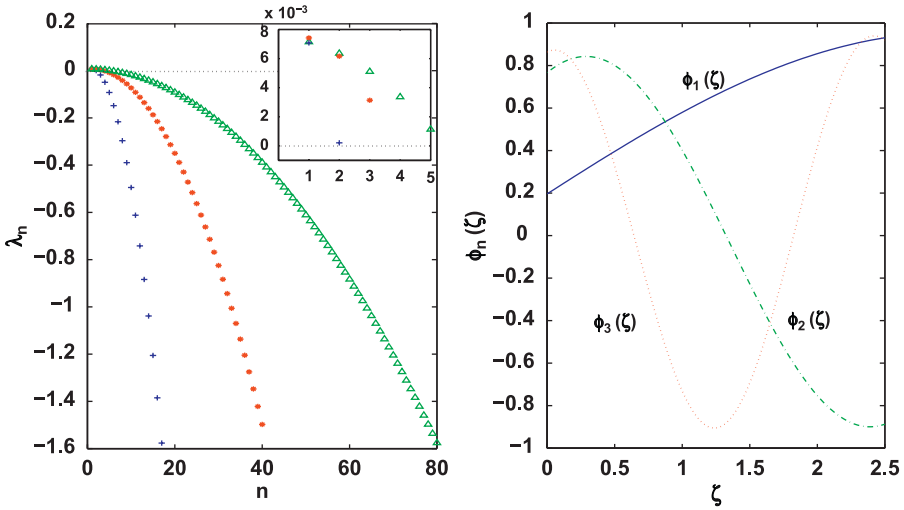

Fig. 2. Left plot: distribution of eigenvalues on the basis of Eq. (20) for different lengths of the cable (1 cm (∗), 2.5 cm (·), 5 cm (△)). Right plot: first three eigenfunctions of unstable eigenmodes of the operator $\mathscr{A}$ given by Eq. (22) for the cable length equal to 2.5 cm.

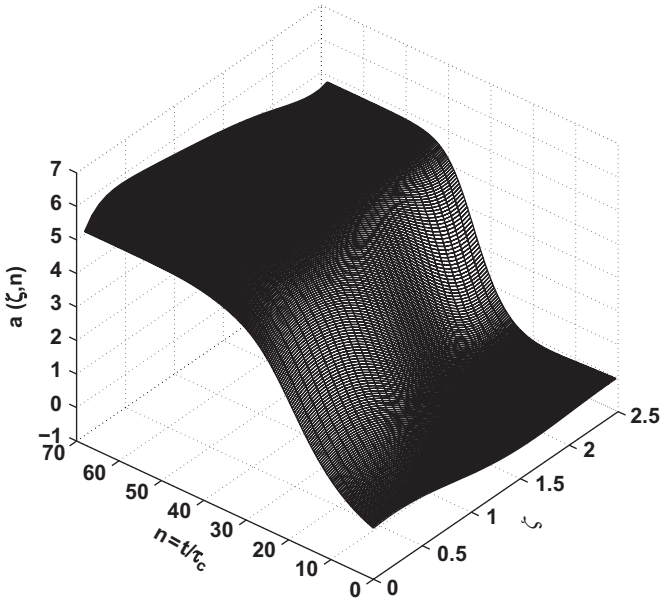

Fig. 3. Open-loop evolution of amplitude of alternans Eqs. (5) and (6).

that an increase in the cable length increases the number of unstable modes of the operator $\mathscr{A}$ which need to be stabilized in order to achieve stabilization along the entire cable length. Moreover, Fig. 2 demonstrates that increase in the cable length promotes more convective nature of the underlying PDE, since the necessary "gap" condition that provides that consecutive stable eigenvalues have a sufficiently large difference among themselves (see the appendix of Christofides, 2001; Temam, 1988), fails to hold. This condition is difficult to satisfy in systems with strong convective terms and/or a small diffusion parameter.

The parabolic PDE of Eqs. (5) and (6) is linearized around the spatially uniform unstable steady state $a(\zeta,0)=0$ and the integral term is neglected in order to allow for LQR controller synthesis. A high-order finite-dimensional approximation of the infinite-dimensional abstract boundary/distributed control problem given by Eq. (17) is first obtained by considering 39 eigenfunctions $a(\zeta,t)=\sum_{i=1}^{39} a_i(t)\phi_i(\zeta)$, and it is given by

$$\dot{a}^e(t)=\bar{\mathscr{A}}^e a^e(t)+\bar{\mathscr{B}}^e\tilde{u}(t) \tag{29}$$

$$y_i(t)=\bar{\mathscr{C}}^e a^e(t) \tag{30}$$

where $\bar{\mathscr{A}}^e$, $\bar{\mathscr{B}}^e$ and $\bar{\mathscr{C}}^e$ are matrices of the following dimensions (40 × 40), (40× (# of spatially distributed actuators)), ((# of spatially distributed sensors) ×40), respectively, with four sensors used at $c(\zeta,\zeta_{ci})=(1/2\varepsilon)1_{[\zeta_{ci}-\varepsilon,\zeta_{ci}+\varepsilon]}(\zeta)$, where ζ_{ci} = [0.0501 1.0772 1.6533 2.3046], while spatially distributed mechanical actuation $b_d(\zeta,\zeta_{d_i})=(1/2\varepsilon)1_{[\zeta_{d_i}-\varepsilon,\zeta_{ci}+\varepsilon]}(\zeta)$ is placed at ζ_{d_i} = [1.6250 2.2250]. Standard Galerkin method is performed (see for details Christofides, 2001), where modal finite-dimensional approximation of Eqs. (5) and (6) is obtained by taking weighted inner product on $L_2(0,l)$ with adjoint eigenfunctions $(a(\zeta,t),\phi_j^*(\zeta))_{w/D_a^2,L_2}$. Function $B(\zeta)\in\mathscr{D}(\mathscr{F})$ is selected to satisfy the following condition $\mathscr{B}Bu(t)=u(t)$ and it is chosen to be $B(\zeta)=\zeta-(1/2l)\zeta^2$. In the extended space $\mathscr{D}(\mathscr{A}^e)=\mathscr{D}(\mathscr{A})\bigoplus U$, the entries of finite-dimensional matrices $\bar{\mathscr{A}}^e$, $\bar{\mathscr{B}}^e$ and $\bar{\mathscr{C}}^e$ are calculated as follows:

$$(\mathscr{F}B)_n=\left(-\frac{D_a^2}{l}-w\left(1-\frac{1}{l}\zeta\right)+\sigma\left(\zeta-\frac{1}{2l}\zeta^2\right),\phi_n^*(\zeta)\right)_{w/D_a^2,L_2}$$

$$B_n=\left(\zeta-\frac{1}{2l}\zeta^2,\phi_n^*(\zeta)\right)_{w/D_a^2,L_2}$$

$$B_{dn}=(b_d(\zeta,\zeta_{ci}),\phi_n^*(\zeta))_{w/D_a^2,L_2}$$

$$C_{in}=\left(\left(c(\zeta,\zeta_{ci}),\zeta-\frac{1}{2l}\zeta^2\right);(c(\zeta,\zeta_{ci}),\phi_n(\zeta))\right)_{w/D_a^2,L_2}$$

for $n\geqslant 1$ and $i=1,\ldots,4$. Note that when the nonlinear and integral terms are considered, they can be computed within the Galerkin-discretization scheme as follows:

$$\mathscr{G}_n(t)=(ga(\zeta,t)^3,\phi_n^*(\zeta))_{w/D_a^2,L_2}$$

$$\mathscr{L}_n(t)=\left(\frac{1}{\Lambda}\int_0^l a(\bar{\zeta},t)\,\mathrm{d}\bar{\zeta},\phi_n^*(\zeta)\right)_{w/D_a^2,L_2}$$

To construct the linear model used for controller design, the first four unstable modal states of the model of Eq. (29) are considered

Author's personal copy

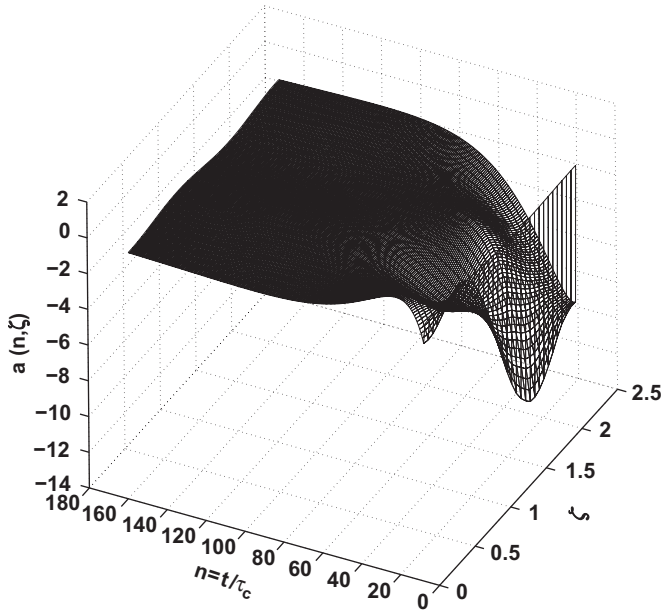

Fig. 4. Boundary/distributed stabilization of the linearized alternans amplitude PDE under the state-feedback control law $\bar{u}(t) = -Ka_u^e(t)$, where $a(\zeta,t) = \sum_i^{39} a_i(t)\phi_i(\zeta)$ and with initial condition $a_{u2}^e(0) = 0.4$, $a_{u3}^e(0) = 0.15$ and $a_{u4}^e(0) = 0.35$.

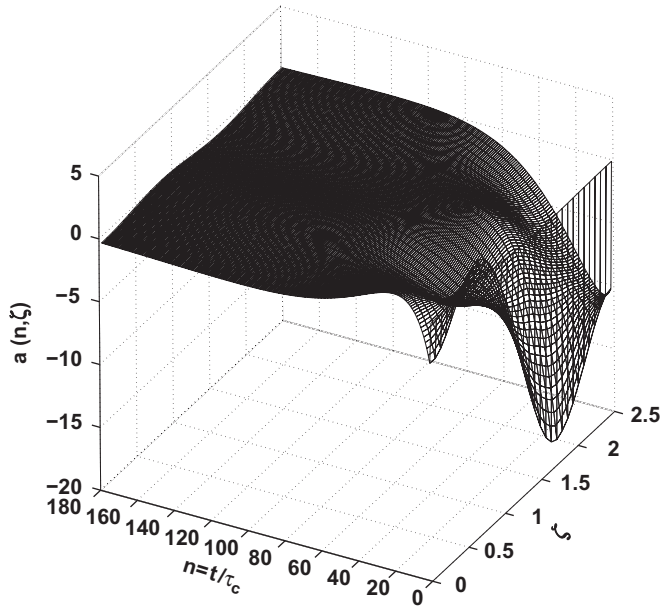

Fig. 5. Boundary/distributed stabilization of the linearized alternans amplitude PDE under linear output-feedback control, where $a(\zeta,t) = \sum_i^{39} a_i(t)\phi_i(\zeta)$ and with initial condition $a_{u2}^e(0) = 0.21$, $a_{u3}^e(0) = 0.4$ and $a_{u4}^e(0) = 0.2$.

as follows:

$$a_u^e(t) = [u(t); p_1(t); p_2(t); p_3(t)]$$

with associated matrices which are of appropriate dimensions (4×4) in the case of

$$\bar{\mathscr{A}}_u = [0\ 0\ 0\ 0; (\mathscr{F}B)_1\ \lambda_1\ 0\ 0; (\mathscr{F}B)_2\ 0\ \lambda_2\ 0; (\mathscr{F}B)_3\ 0\ 0\ \lambda_3]$$

(4×2) in the case of $\bar{\mathscr{B}}_u = [I\ 0; -B_1\ B_{d1}; -B_2\ B_{d2}; -B_{d3}]$, with B_{d1}, B_{d2}, B_{d3} being (2×1) matrices, and (4×4) in the case of $\bar{\mathscr{C}}_u = [B(\zeta_{ci}); \phi_1(\zeta_{ci}); \phi_2(\zeta_{ci}); \phi_3(\zeta_{ci})]$, with $\bar{u}(t) = [\tilde{u}(t)\ u_d(t)]'$ and $\tilde{u}(t)$ being derivative of $u(t)$. The LQR regulator control law $\bar{u}(t) = -Ka_u^e(t)$ is the solution of the following optimization problem:

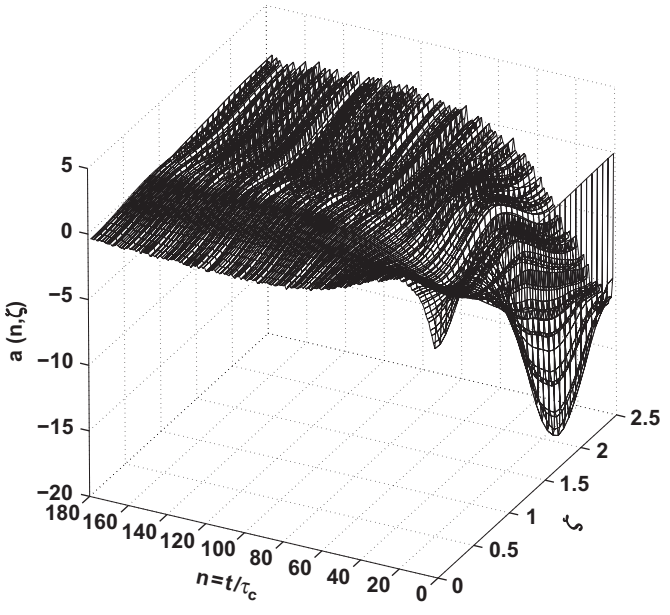

Fig. 6. Boundary/distributed stabilization of the linearized alternans amplitude PDE under linear output-feedback control, with measurement noise $\varrho(t) \leqslant 0.001$ and with initial condition $a_{u2}^e(0) = 0.21$, $a_{u3}^e(0) = 0.4$ and $a_{u4}^e(0) = 0.2$.

$$\min_{\bar{u}} \quad J(a_u^e(0); \bar{u}) = \int_0^\infty (a_u^e(t)' Q a_u^e(t) + \bar{u}(t)' R \bar{u}(t))\,\mathrm{d}t \tag{31}$$

$$\text{s.t.} \quad \dot{a}_u^e(t) = \bar{\mathscr{A}}_u a_u^e(t) + \bar{\mathscr{B}}_u \bar{u}(t) \tag{32}$$

which yields the following stabilizing gain:

$$K = \begin{pmatrix} 3.136 & 0.7755 & 0.1967 & 0.06276 \\ 1403.5 & 24.1305 & 66.790 & 59.2839 \\ 995.30 & 38.431 & 123.71 & -61.4311 \end{pmatrix}$$

that places the unstable eigenmodes of the four-dimensional closed-loop system at the following locations $\lambda_{cl} = [-4.0508\ -0.0074\ -0.0062\ -0.0032]$ for the following values of matrices $Q^e = [q_u\ 0;\ 0\ q_a I]$, where $q_a = 0.01$ and I is the unitary matrix and $q_u = 0.0001$, where $R = \mathrm{diag}\{R_u, R_{ud}\}$ with $R_u = 100$ and $R_{ud} = 0.0001$. Furthermore, the gain of the Luenberger observer of Eq. (28) is calculated as the gain that places the observer eigenvalues at $\lambda_{\mathscr{L}C} = \lambda_{cl} - 2.5$ in order to ensure faster convergence of the observer dynamics compared to the closed-loop system dynamics under state feedback control. The control law $\tilde{u}(t) = -Ka_u^e(t)$ is first applied to the linear finite-dimensional approximation of Eqs. (29) and (30) with 39 eigenfunctions and the solution is obtained by integrating the closed-loop system by an explicit Euler integration scheme where the time step is taken as $\Delta t = (1/4 \max|\mathrm{eig}\{\Omega(\mathscr{A})^e\}|)$ so that numerical stability is ensured.

Complementary with Fig. 4 is Fig. 8 that shows the evolution of the control $u(t)$ applied at the boundary $\zeta = 0$ and spatially distributed $u_d(t)$ at $\zeta_{d_i} = [1.6250\ \ 2.2250]$. In the simulation study, it is demonstrated that the PDE state close to the boundary where control is applied undergoes large variations in the magnitude even for a relatively small excursion of initial conditions, which is due to the necessity to have the three unstable modes stabilized, see Figs. 4–8. In the case of linear output-feedback control with four point measurements, the successful stabilization of alternans is achieved in a similar manner as in the case of state-feedback stabilization, see Fig. 5. As expected, it is observed that the state-feedback controller

Author's personal copy

slightly outperforms the output-feedback controller, see Figs. 5–8. In Fig. 8 both dashed and solid lines converge to the same trajectory, as it takes initially some time for the state estimate to converge to the actual state.

In addition, when the impact of noisy measurements is included in the output-feedback controller implementation, our simulation studies, using the linearized PDE model, demonstrate that even a very small noise level results in substantial deviation of the state $a(n,\zeta)$ from the zero solution. Namely, for noise of magnitude $\varrho(t)\leqslant 0.001$ that is directly added to $y(t)$ in Eq. (28), we observe, see Figs. 6 and 8 (dotted and dashed lines of the input profiles almost coincide as the difference is only due to the additive measurement noise), that $a(n,\zeta)$ behaves like a near standing wave in space which oscillates around $a(n,\zeta)=0$ with respect to time. This strongly advocates and confirms that the current realization of noisy stabilizing protocols cannot inherently stabilize (i.e., set $a(n,\zeta)=0$) alternans due to high sensitivity to noisy measurements used in the feedback controller.

Finally, in Fig. 7, it can be seen that the stabilization of the spatially uniform unstable steady state of the full nonlinear model of Eqs. (5) and (6) under the linear LQR control law is achieved. This result makes sense since essentially both the nonlinear and integral terms provide a stabilizing effect on the amplitude of alternans, which is also manifested in the faster convergence of the applied boundary and spatially distributed inputs to zero, see Fig. 8.

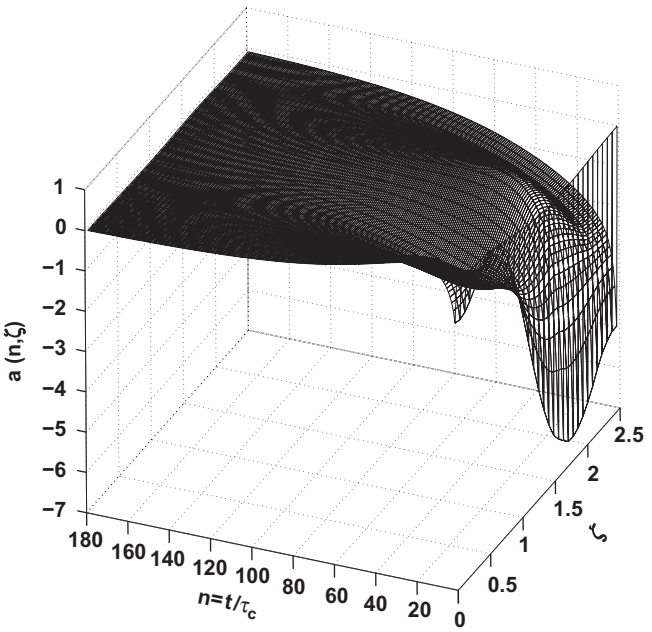

Fig. 7. Boundary/distributed stabilization of the nonlinear alternans amplitude PDE given by Eqs. (5) and (6) under the linear LQR state-feedback control law $\tilde{u}(t)=-Ka(t)$, and with initial condition $a^e_{ti2}(0)=0.21$, $a^e_{ti3}(0)=0.4$ and $a^e_{ti4}(0)=0.2$.

5. Summary

The work focused on mixed boundary/spatially distributed control of the amplitude of alternans parabolic PDE using optimal control methods. This problem arises in the context of stabilization of cardiac alternans using mechano-electric feedback. The proposed control problem formulation and the performance and robustness of the closed-loop system were studied through simulations.

Acknowledgment

Financial support from AHA (American Heart Association) Post-Doctoral Grant Award 0725121Y for Stevan Dubljevic is gratefully acknowledged.

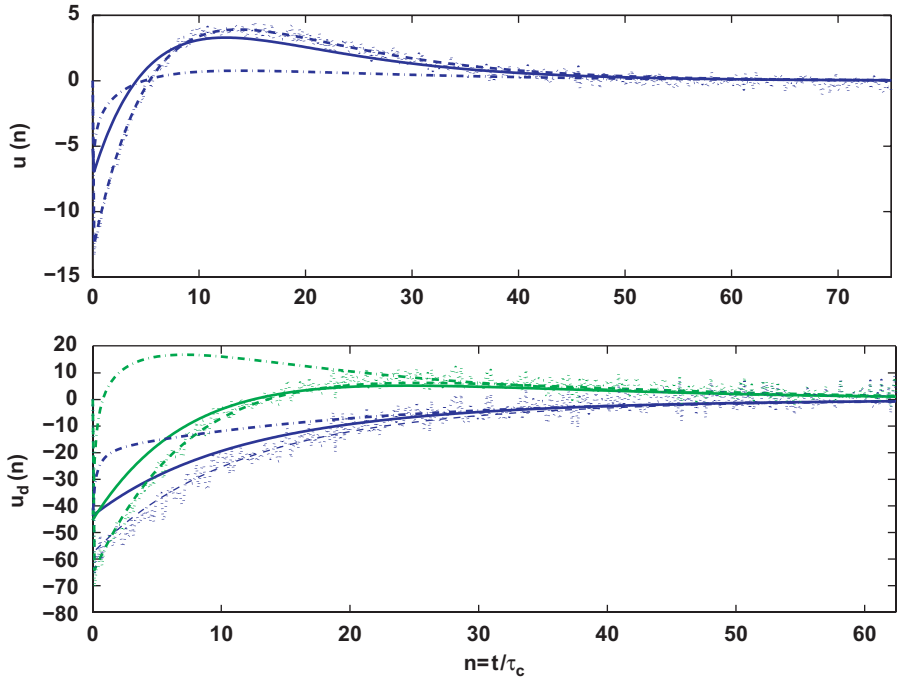

Fig. 8. Optimal control input computed by the state-feedback control law (solid-line—boundary input $u(n)$ and distributed input $u_d(n)$), by the output-feedback control law (dashed-line—boundary input $u(n)$ and distributed input $u_d(n)$), by the output-feedback control law with the additive noise (dotted-line—boundary input $u(n)$ and distributed input $u_d(n)$), applied to the linearized alternans amplitude PDE, and optimal control input under the LQR state-feedback control law applied to Eqs. (5) and (6) (dashed-dotted-line—boundary input $u(n)$ and distributed input $u_d(n)$).

Author's personal copy

References

Antoniades, C., Christofides, P.D., 2001. Integrating nonlinear output feedback control and optimal actuator/sensor placement in transport-reaction processes. Chemical Engineering Science 56, 4517–4535.

Armaou, A., Demetriou, M., 2006. Optimal actuator/sensor placement for linear parabolic pdes using spatial H_2 norm. Chemical Engineering Science 61, 7351–7367.

Balas, M.J., 1978. Active control of flexible systems. Journal of Optimization Theory and Applications 25, 415–436.

Beeler, G.W., Reuter, H., 1977. Reconstruction of the action potential of ventricular myocardial fibers. Journal of Physiology 268, 177–210.

Bers, D.M., 2001. Excitation–Contraction Coupling and Cardiac Contractile Force. Kluwer Academic Publishers, Dordrecht.

Boskovic, D.M., Kristc, M., Liu, W., 2001. Boundary control of an unstable heat equation via measurement of domain-averaged temperature. IEEE Transactions on Automatic Control 46, 2022–2028.

Byrnes, C.I., Gilliam, D.S., Isidori, A., Shubov, V.I., 2004. Static and dynamic controllers for boundary controlled distributed parameter systems. In: Proceedings of the 43rd IEEE Conference on Decision and Control, pp. 3324–3325.

Calaghan, S.C., Belus, A., White, E., 2003. Do stretch-induced changes in intracellular calcium modify the electrical activity of cardiac muscle? Progress in Biophysics and Molecular Biology 82, 81–95.

Chakravarti, S., Ray, W.H., 1999. Boundary identification and control of distributed parameter systems using singular functions. Chemical Engineering Science 54, 1189–1204.

Christini, D.J., Riccio, M.L., Culianu, C.A., Fox, J.J., Karma, A., Gilmour, R.F., 2006. Control of electric alternans in canine cardiac purkinje fibers. Physical Review Letters 96, 104101.

Christofides, P.D., 2001. Nonlinear and Robust Control of PDE Systems: Methods and Applications to Transport-Reaction Processes. Birkhäuser, Boston.

Cross, M.C., Hohenberg, P.C., 1993. Pattern formation outside of equilibrium. Reviews of Modern Physics 65, 851.

Curtain, R.F., Zwart, H., 1995. An Introduction to Infinite-Dimensional Linear Systems Theory. Springer, New York.

Dochain, D., 2001. State observation and adaptive linearizing control for distributed parameter (bio)chemical reactors. International Journal of Adaptive Control and Signal Processing 15, 633–653.

Dubljevic, S., Christofides, P.D., 2006a. Predictive control of parabolic PDEs with boundary control actuation. Chemical Engineering Science 61, 6239–6248.

Dubljevic, S., Christofides, P.D., 2006b. Predictive output feedback control of parabolic PDEs. Industrial and Engineering Chemistry Research 45, 8421–8429.

Dubljevic, S., El-Farra, N.H., Mhaskar, P., Christofides, P.D., 2006. Predictive control of parabolic PDEs with state and control constraints. International Journal of Robust and Nonlinear Control 16, 749–772.

Dubljevic, S., Lin, S.-F., Christofides, P.D., 2008. Studies on feedback control of cardiac alternans. Computers and Chemical Engineering 32, 2086–2098.

Echebarria, B., Karma, A., 2002a. Instability and spatiotemporal dynamics of alternans in paced cardiac tissue. Physical Review Letters 88, 208101.

Echebarria, B., Karma, A., 2002b. Spatiotemporal control of cardiac alternans. Chaos 12, 923–930.

Emirsjlow, Z., Townley, S., 2000. From PDEs with boundary control to the abstract state equation with an unbounded input operator: a tutorial. European Journal of Control 6, 27–49.

Fattorini, H.O., 1968. Boundary control systems. SIAM Journal on Control 6, 349–385.

Friedman, A., 1976. Partial Differential Equations. Holt, Rinehart & Winston, New York.

Hagen, G., Mezic, I., 2003. Spillover stabilization in finite-dimensional control and observer design for dissipative evolution equation. SIAM Journal on Control and Optimization 42, 746–768.

Kohl, P., Ravens, U., 2003. Cardiac mechano-electric feedback: past, present, and prospect. Progress in Biophysics and Molecular Biology 82, 3–9.

Kohl, P., Hunter, P., Noble, D., 1999. Stretch-induced changes in heart rate and rhythm: clinical observations, experiments and mathematical models. Progress in Biophysics and Molecular Biology 71, 91–138.

Lin, S.-F., Dubljevic, S., 2007. Pacing real-time spatiotemporal control of cardiac alternans. In: Proceedings of the American Control Conference, New York City, NY, pp. 600–606.

Ray, W.H., 1981. Advanced Process Control. McGraw-Hill, New York.

Solovyova, O.E., Vikulova, N.A., Konovalov, P.V., Kohl, P., Markhasin, V.S., 2004. Mathematical modeling of mechano-electric feedback in cardiomyocytes. Russian Journal of Numerical Analysis and Mathematical Modelling 4, 331–351.

Temam, R., 1988. Infinite-Dimensional Dynamical Systems in Mechanics and Physics. Springer, New York.

Triggiani, R., 1980. Boundary feedback stabilization of parabolic equations. Applied Mathematics and Optimization 6, 201–220.

Willems, J.C., 1971. Least squares stationary optimal control and the algebraic Riccati equation. IEEE Transactions on Automatic Control 6, 621–634.